EFDA–JET–CP(12)06/07

A. Kallenbach, M. Bernert, R. Dux, T. Eich, C. Giroud, A. Herrmann,
J.W. Hughes, M. Lehnen, B. Lipschultz, A. Loarte, G. Maddison, F. Reimold,
M. Reinke, J. Schweinzer, B. Sieglin, M. Wischmeier, S. Wolfe,
ASDEX Upgrade Team, Alcator Team, and JET EFDA contributors

Multi-Machine Comparisons of Divertor Heat Flux Mitigation by Radiative Cooling with Nitrogen

Multi-Machine Comparisons of Divertor Heat Flux Mitigation by Radiative Cooling with Nitrogen

A. Kallenbach[1], M. Bernert[1], R. Dux[1], T. Eich[1], C. Giroud[2], A. Herrmann[1], J.W. Hughes[3], M. Lehnen[4], B. Lipschultz[3], A. Loarte[5], G. Maddison[2], F. Reimold[1], M. Reinke[3], J. Schweinzer[1], B. Sieglin[1], M. Wischmeier[1], S. Wolfe[3], ASDEX Upgrade Team, Alcator Team, and JET EFDA contributors*

JET-EFDA, Culham Science Centre, OX14 3DB, Abingdon, UK

[1]Max Planck Institute for Plasma Physics, EURATOM Association, Garching, GERMANY
[2]EURATOM-CCFE Fusion Association, Culham Science Centre, OX14 3DB, Abingdon, OXON, UK
[3]Massachusetts Institute of Technology, Plasma Science and Fusion Center, Cambridge, USA
[4]IEK-Plasmaphysik, Forschungszentrum Jülich, Association EURATOM-FZJ, Jülich, Germany
[5]ITER Organization, Route de Vinon sur Verdon, 13115 Saint Paul Lez Durance, France
** See annex of F. Romanelli et al, "Overview of JET Results", (24th IAEA Fusion Energy Conference, San Diego, USA (2012)).*

Preprint of Paper to be submitted for publication in Proceedings of the 24th IAEA Fusion Energy Conference (FEC2012), San Diego, USA 8th October 2012 - 13th October 2012

ABSTRACT

The exhaust characteristics and performance of nitrogen seeded H-mode discharges in Alcator C-Mod, ASDEX Upgrade and JET-C (carbon plasma facing components) have been analysed by regression analysis of plasma parameters relevant for power exhaust and simple analytic models. The highest divertor radiation levels observed lie around or below the maximum level expected from simple analytic considerations, which suggest a P/R metric or size scaling. Regression of the divertor radiation versus Z_{eff}, the divertor neutral pressure, the expected power width and the major radius suggest exponents $R^{1.5}$ for the full dataset including unseeded, low intrinsic divertor radiation levels and $R^{1.1}$ if only nitrogen seeded discharges are taken into account. Extrapolated ITER divertor radiation levels for $\delta Z_{eff} = 1$ by nitrogen are 75 and 25MW if a small power width of 1.6mm mapped to the outer midplane is assumed at the entrance of the radiating zone. The fits suggest that a higher neutral pressure in the JET divertor would be beneficial for a higher radiation level. Normalised confinement improves with β_N, suggesting improvements for higher heating powers for C-Mod and JET.

1. INTRODUCTION

Due to the absence of carbon as intrinsic low-Z radiator, and tight limits for the acceptable power load on the divertor target, ITER will rely on impurity seeding for radiative power dissipation and for generation of partial detachment. The ITPA group for integrated operational scenarios (IOS) initiated cross-machine studies of impurity seeded scenarios under conditions which should be as similar to ITER as possible. Since ELM mitigation will be mandatory in ITER, the seeding scenario has finally to be integrated with ELM mitigation techniques. Currently, the phenomenology of the plasma response to impurity seeding appears quite different in different devices, as does the response to magnetic perturbations aimed towards ELM mitigation. This paper presents a comparison of the effects of nitrogen seeding in Alcator C-Mod, ASDEX Upgrade (AUG) and JET-C (with carbon plasma facing components) regarding energy confinement variation and the rise in impurity content which is required to achieve a certain divertor radiation level. Due to quite different divertor geometries and the underlying complicated physics, a strict machine size scaling or metric of seeding efficiency is hard to establish [1] [2]. Useful trends can be derived from modelling and simple experimental scalings.

In the following, seeding scenarios and simple expectations are compared to observations in the three tokamaks with different levels of nitrogen seeding. Relevant experimental parameters are compared in scaling relations for a rough, empirical extrapolation to ITER.

2. SEEDING SCENARIOS AND SCALING PARAMETERS

To avoid unacceptable co-deposition of fuel atoms, only recycling impurities are feasible for plasma seeding with the aim to increase radiative losses and facilitate partial detachment. A mix of 2 impurities should be considered for ITER, a low-Z species for divertor radiation and a medium-Z

species for core radiation. Nitrogen is favoured as divertor radiator since it has a high radiative capability at low temperatures which are required to make hydrogenic momentum loss processes effective. For a closed, high recycling divertor with moderate pumping, the impurity puff location is expected to be of minor importance, since the impurity recycling fluxes will dominate the puffed flux. This situation is assumed for AUG, C-Mod, JET and ITER. Different in this respect is DIII-D with the strike point position at the entrance of the pumping slot, where seed species enrichment in SOL and divertor has been achieved by puff and pump [3].

The power dissipation in the divertor is less easily compared between different devices due to quite different divertor geometries and experimental conditions. Dimensionless divertor identity or at least dimensionless scaling experiments for extrapolation to ITER appear not feasible with present day devices. 2D-modelling, on the other hand, suffers from problems in reproducing detachment in present day devices [4] and the not well known scrape-off layer transport.

We compare discharges in different devices with nitrogen seeding for dominant increase of the divertor radiation and detachment support. Deuterium puffing for the achievement of a high deuterium recycling level is an important ingredient to avoid core plasma pollution and for the facilitation of detachment.

3. RADIATION SCALINGS AND EXPECTATIONS FROM SIMPLE ANALYTIC MODELS

A multi-machine scaling for the total radiated power in a tokamak was presented by G. Matthews [5], predicting

$$P_{rad,tot} = 1/7 \quad (Z_{eff} \; - 1) \cdot \; S\bar{n}_e^2, \tag{1}$$

where the total radiated power is given in MW and the line averaged electron density in [1020 m3]. The linear dependence from the plasma surface S suggests a size similarity metric μ R2, however, there is no explicit dependence on the heating power in the Matthews scaling. This scaling did not distinguish main chamber and divertor radiation, but main chamber radiation is supposed to dominate the corresponding data since mostly data from open divertor or limiter machines have been used. Comparing the present data set with Eq. 1 shows substantial deviations, with the total radiated power in AUG about a factor 2 higher than predicted, JET data a factor 2 lower than predicted and C-Mod data a factor 2-5 lower than predicted. A recent comparison of JET-ILW data with Eq. 1 revealed deviations attributed to changing impurity composition and a quite different behaviour of divertor and bulk radiation [6]. In the following, simple physics based analytic expressions for the expected radiation levels will be given.

3.1. MAIN CHAMBER RADIATION

Core radiating, medium-Z impurities are usually close to Coronal ionization equilibrium and the

radiated power density is expected to be reasonably well described by the product $L_z(T_e) \cdot c_z \cdot n^2_e$, where L_z is the radiative loss function and c_z is the corresponding impurity concentration [7]. For identical normalized plasma prole shapes,impurity species and n_e and T_e values, the core radiated power scales with plasma volume, $\propto R^3$. Important parameters for the real radiation power scaling are the not well known size scalings of the temperature and density pedestal widths. Both widths are expected to scale $\propto R^{-0.1}$. Since larger tokamaks have usually a significantly higher pedestal temperature ($T_{e,ped}$ roughly ~ R), the highly emitting zone of medium-Z impurities shrinks with tokamak size resulting in $P_{rad,core} \sim R^{1-2}$ for n_e and c_z kept constant. Finally, the higher absolute T_e in a larger device will shift $L_z(T_e)$ towards lower values. This can be compensated by using an impurity with higher Z, which reduces fuel dilution, but causes higher central radiative losses. Main chamber radiation is not further considered in this work since ITERs proximity to the L-H power threshold will not allow strong core seed radiation. The technical feasibility of a combined core (Ar) and divertor (N) seeding has recently been demonstrated in AUG [8].

3.2. DIVERTOR RADIATION

Estimates of the scaling behaviour of the divertor radiation are uncertain, since substantial deviations from Coronal equilibrium occur and various atomic physics effects contribute. Figure 1 shows tomographic reconstructions of the radiation distribution in nitrogen- and non-seeded discharges in JET-C and AUG, and a JET-ILW example without N. The radiated power density concentrates in a small region around the X-point and in the inner divertor. High radiation is also seen at AUG around the outer strike point. It should be noted that deconvolution of a nitrogen seeded discharge from JET-ILW shows a radiation distribution very similar to the N-seeded JET-C example in figure 1, however a limited bolometric coverage of the outer divertor in JET should be noted in this context. An important player is the divertor detachment, which occurs regularly at least in the inner divertor of D fuelled H-modes. Several processes contribute to detachment, which can so far not be quantitatively reproduced by modelling of present day tokamaks [4]. The recently found approximate independence of the mid-plane power decay length lq from machine size [10] suggests a simple size-scaling model of divertor radiation. Assuming that the main dissipation of power happens in the vicinity of the target plate, the parallel power density in this region may scale as P_{sep}/R. No radial or vertical size increase of the radiating zone are assumed in this simple picture. The P/R scaling is the conservative, most pessimistic assumption for extrapolation to a larger device, higher vales of the size exponent will result in an easier achievement of a certain radiative power loss. An important question is the possible saturation of divertor radiation with increasing impurity content [11]. This effect is expected from simple analytic 1-d modelling of divertor radiation and related to a steepening of T_e along the field lines caused by the reduced parallel heat conductivity due to increased Z_{eff}. The steepening of T_e causes a shrinking of the radiative layer, and thus a reduction of the radiative efficiency. The maximum radiated power flux along a field line Q^{max}_{rad} is calculated analytically from the radiative loss function Lz [11], taking the Z_{eff} dependence of the heat conductivity from [12]:

$$Q_{rad}^{max} = n_{e,mid} T_{e,mid} \, (2\kappa_0 f_z \int_{T_{e,tar}}^{T_{e,mid}} L_z(T_e) \, T_e^{0.5} \, 5/(4 + Z_{eff}(T_e)) \, dT_e)^{0.5} \, [W/m^2] \qquad (2)$$

Here, f_z is the concentration of the impurity species considered, the effective charge Z_{eff} is calculated as a function of the local T_e along the field line from ionization balance. For divertor conditions, the value of L_z is enhanced by deviations from Coronal equilibrium. This can be described by a parameter net, which represents the ratio of impurity residence and ionisation times. To estimate the maximum total divertor radiation from Eq.2, we multiply Q_{rad}^{max} with the number of divertor legs, n=2, and the area of a toroidal ring situated at the outer midplane with the circumference $2\pi(R+a)$ and the power width λ_q, resulting in

$$P_{rad,\,div}^{max} = 4\pi(R + a)\lambda_q Q_{rad}^{max} \qquad (3)$$

Figure 2a shows the maximum achievable divertor radiation as a function of the midplane separatrix temperature for a nitrogen seeded case for typical AUG like parameters in practical units. The conditions can be easily adapted to the C-Mod and JET cases using Eqs.2 and 3.

4. DATABASE

An experimental database has been collected from well diagnosed discharges with different nitrogen seeding levels in AUG (28 slices out of 18 ELMy H-mode discharges [8]), C-Mod (69 slices / 5 EDA H-mode discharges [13]) [14] and JET-C (7 slices / 7 ELMy H-mode discharges [15]). The C-Mod and JET data represent discharges with quite similar conditions (q_{95} = 3.5 for JET and 4 for C-Mod) and contain mainly scans of nitrogen D gas fuelling at similar heating powers. AUG data contain as well variations of plasma current and heating power, q_{95} = 3.9-4.8. Z_{eff} data are taken from bremsstrahlung measurements in AUG and JET, for C-Mod Z_{eff} calculated from proles assuming neoclassical plasma resistivity with bootstrap current correction has been selected. The Z_{eff} values from bremsstrahlung for C-Mod are typically higher by 20% for the present data set, which could be due to blending spectral lines. For AUG, Z_{eff} values are used which have been averaged along a non-central interferometer chord, since Z_{eff} proles are hollow and the divertor impurity content is supposed to correlate with the peripheral Z_{eff} values. Figure 3 gives a characterization of the present data base. An approximate power balance is shown in figure 3a as the comparison of the heating power with the sum of main chamber radiated power, divertor radiated power and the power onto the outer target from thermography. Reasonable agreement is obtained for AUG and C-Mod, where the radiated measured power accounts for any ELM radiation and mostly radiative power load is expected on the inner target. Some excess power in the balance may be caused by radiative power load on the outer target and general uncertainties. A considerable fraction of power 40% is not accounted for in JET by this ansatz, which may be explained by the omission of ELM power losses and some not accounted power probably released at the main chamber walls [16]. Figure 3b

shows main chamber versus the divertor radiated power fraction. The highest radiation levels are obtained in C-Mod, the lowest values are observed in JET. To identify a machine size dependence, the dependence of the divertor radiation on density or divertor neutral pressure and impurity content have to be determined. No reliable impurity concentration measurement in the divertor is available, therefore the latter is approximated by Z_{eff} measured in the core plasma. The results shown in figure 2a can be used to estimate the maximum divertor radiated power for the database. The power width λ_q , which is evaluated at the entrance of the radiating zone and mapped to the outer midplane is calculated using Eq.5 from [12], which is about 2 the experimental lq scaling in [10]. The factor 2 has been introduced to take into account a broadening of the heat flux towards the radiating zone. This broadening appears in the quantity λ_{int} as discussed in [10] and is not easily scaled to ITER [17]. Typical resulting values of λ_q are 4mm for AUG, 3.2mm for JET and 2mm for C-Mod, the corresponding ITER value is 1.6mm. Further, an upstream separatrix T_e of 100eV and a midplane separatrix density of 1/3 of the typical line-averaged density are assumed for the three tokamaks. The maximum radiated powers for $n_e \tau = 1$ are shown in figure 2b and compared to the measurements. The achieved radiation levels lie well below the maximal ones calculated, however, the highest radiation levels observed come close. The maximum divertor radiated power for ITER ($T_{e,mid} = 160$eV, $n_{e,mid} = 3.5\times10^{19}$ m^{-3}) for nitrogen seeding results in 25MW, which is low compared to the heat flux into the divertor of 100MW expected for the standard case [18, 19]. The low value is among others caused by the small value of λ_q assumed. Equation 3 in principle corresponds to P/R as the correct metric for size scalings. This, however, is modified by the insufferably low λ_q caused by the high plasma current. The ITER value of 1.6 mm used here is the lower limit of expectation, recent analysis suggests a higher value of lint in ITER [17] and thus a higher power width at the radiating region. While the model described above should at least show the right trends, one should keep in mind that the absolute numbers are uncertain since effects like charge exchange and recombination have been neglected. This is in particular true for the inner divertor, where these effects are predominant.

As a complement to the simple analytical considerations given above, regression analysis of the divertor radiated power and the peak heat flux has been performed. Equation 3 gives the result, which is graphically shown in figure 4a.

$$P_{rad,\,div} = 72\, p_{0,div}^{0.6}\, (Z_{eff} - 1)^{0.43}\, R^{1.5}\, \lambda_q^{0.64} \quad [MW],\ [Pa],\ [m],\ [m] \tag{4}$$

$p_{0.div}$ is the neutral pressure measured in the divertor PFR region. For the power width λ_q again the upstream value from Goldstons drift model is used. Evaluating equation 4 for ITER with the parameters stated above and $Z_{eff} = 2$ and $p_{0,div} = 10$Pa [19] results in a predicted divertor radiation level of 75MW. The upstream power width has been included because it is plausible that this parameter is important for the radiating volume and thus the radiated power. Since the fit shown in figure 4a shows pronounced deviations for discharges without N seeding/very low divertor radiation, the fit has been repeated taking only N-seeded discharges with enhanced divertor radiation into

account (removing 7 AUG and 1 JET entry). $Z_{eff}-1$ becomes so a better measure for the nitrogen concentration. The fit obtained is shown in figure 4b:

$$P_{rad,div,\,N\,only} = 1720\; p_{0,div}^{0.47}\; (Z_{eff}-1)^{0.31} R^{1.095}\; \lambda_q^{1.148}\; [MW], [Pa], [m], [m] \qquad (5)$$

Now, the dependence of major radius R and (assumed) power width lq is almost linear as expected in the simple analytical radiation model. The prediction for ITER comes down to 25MW divertor radiation. In view of the fact that the value of λ_q used for ITER will be corrected upwards by about a factor of 2 due to the higher power width broadening [17], the low predicted radiation level causes no big concerns. The relatively low divertor radiation in the JET discharges is mainly caused by the low neutral D pressure.

4.1. IMPACT ON ENERGY CONFINEMENT

The impact of impurity seeding on energy confinement is quite different in different tokamaks. In Alcator C-Mod, a reduction of pedestal temperature and normalized confinement is observed when the power flux through the separatrix is reduced towards the L-H threshold power, P_{LH}, resulting in H_{98} decreasing from $H_{98} \approx 1.2$ to 1 for $P_{sep}/P_{LH} = 1$ [20] [13]. In AUG, improvement of confinement is seen at higher values of P_{sep}/P_{LH} which correlates with increasing Z_{eff} due to N seeding and increased pedestal pressure [21]. Ar seeding has no pronounced effect on energy confinement in AUG at least at high heating powers [22], despite the radiation of Ar being predominantly from inside the separatrix. In JET-C with a carbon divertor, a reduction of H_{98} was always observed during impurity seeding [23] [15]. It should be noted that in JET-ILW, an increase of H_{98} with increasing N seeding was recently observed for high triangularity discharges [24].

Figure 5 compares the behaviour of normalised energy confinement in our database. A rise of H_{98} is observed in figure 5a when the heating power is increased w.r.fit. the L-H power threshold [25], the same is seen when we use the radiation corrected power flux into the divertor (Fig.5b). The data from all 3 tokamaks is compatible to a rise in H_{98} with increasing β_N (Fig.5c), reminiscent of previous findings in hybrid discharges [26]. Since there is no big variation of heating power or other parameters entering in the H_{98} calculation in the data sets from JET and C-Mod, the shown trend is just a co-linearity for these devices since the plasma energy enters linearly both into H98 and β_N. The AUG data contain a substantial power variation, and suggest that a high β_N may be necessary for a high H_{98} for these experimental conditions.

DISCUSSION AND CONCLUSIONS

The comparison of the effect of nitrogen seeding in the tokamaks Alcator C-Mod, ASDEX Upgrade and JET has revealed a number of similarities and differences.

Energy confinement is reduced when core radiation reduces the stored energy. Whether the latter effect occurs depends on the spatial distribution of the radiation and not well understood transport

effects. e.g., on high β_N discharges in AUG, core radiation by Ar does not lead to confinement degradation, while this is clearly observed on C-Mod [20]. This difference calls for the inclusion of radiative losses in first principle transport calculations.

Within considerable uncertainties, the ratio of separatrix power flux and the major radius, P_{sep}/R, appears as an appropriate parameter for the required seeding effort to achieve moderate peak heat flux, albeit some differences are expected between the effects of main chamber and divertor radiation. The maximum divertor radiated power calculated from a simple analytical radiation model is consistent with the highest divertor radiation levels in the database presented. AUG reaches just the corresponding value, but no saturation of divertor radiation has been observed in experiment so far. The quite low radiative efficiency of nitrogen in the JET divertor (figure 4c) is attributed to the low neutral D pressure. It is plausible that momentum loss processes like charge exchange and recombination increase the radiation limit. Therefore, the quite low expectation of 25MWfor ITER has to be considered as a conservative/pessimistic lower bound. Predictions for the ITER radiation level from power law scalings are 25 and 75MW, but substantial uncertainties have to be considered.

Despite considerable differences in machine responses to impurity seeding, a reduction of normalized confinement with decreasing separatrix power flux is noticeable. Empirically, the closeness to the L-H threshold power allows a reasonable normalisation, but it is unclear whether the underlying physics is connected to the L-H transition. The close correlation of H-factor and β_N observed suggests that increasing the heating power in C-Mod and JET seeded scenarios would allow for higher values of H_{98}, as seen in AUG. This would not hold for the ITER standard scenario since operation is foreseen at a relatively low $\beta_N = 1.8$, but may become favourable for the development of advanced scenarios in ITER.

Finally, the radiative seeding has to be embedded with an ELM mitigation technique. No problems are expected for ELM pacemaking by pellets [27]. On the other hand, no clear picture is known yet for the interplay with ELM mitigation by magnetic perturbations [28] [29].

ACKNOWLEDGEMENT

This work was supported by EURATOM and carried out within the framework of the European Fusion Development Agreement. The views and opinions expressed herein do not necessarily reflect those of the European Commission. The views and opinions expressed herein do not necessarily reflect those of the ITER Organization.

REFERENCES

[1]. Kotschenreuther, M. et al., Physics of Plasmas **14** (2007) 072502.
[2]. Kotschenreuther, M. et al., Nuclear Fusion **50** (2010) 035003.
[3]. Petrie, T. et al., Nuclear Fusion **48** (2008) 045010.
[4]. Wischmeier, M. et al., Journal of Nuclear Materials **415** (2011) S523.

[5]. Matthews, G.F. et al., Journal of Nuclear Materials **241–243** (1997) 450.
[6]. Devynck, P. et al., 39th EPS Conference (2012), http://ocs.ciemat.es/epsicpp2012pap/pdf/P4.012.pdf .
[7]. Kallenbach, A. et al., Journal of Nuclear Materials **415** (2011) S19.
[8]. Kallenbach, A. et al., 39th EPS Conference (2012), http://ocs.ciemat.es/epsicpp2012pap/pdf/P1.083.pdf
[9]. Fuchs, J. C. et al., Journal of Nuclear Materials **290–293** (2001) 525.
[10]. Eich, Fit. et al., Physical Review Letters **107** (2011) 215001.
[11]. Post, D. et al., Physics of Plasmas **2** (1995) 2328.
[12]. Goldston, R., Nuclear Fusion **52** (2012) 013009.
[13]. Hughes, J. et al., Nuclear Fusion **51** (2011) 083007.
[14]. Loarte, A. et al., Physics of Plasmas **18** (2011) 056105.
[15]. Giroud, C. et al., Nuclear Fusion **52** (2012) 063022.
[16]. Eich, Fit. et al., Plasma Physics and Controlled Fusion **49** (2007) 573.
[17]. Eich, Fit. et al., ITR/1-1, this conference .
[18]. Kukushkin, A.S. et al., Nuclear Fusion **43** (2003) 716.
[19]. Pacher, H. et al., Journal of Nuclear Materials **415** (2011) S492.
[20]. Reinke, M. et al., Journal of Nuclear Materials **415** (2011) S340.
[21] . Schweinzer, J. et al., Nuclear Fusion **51** (2011) 113003.
[22]. Kallenbach, A. et al., Journal of Nuclear Materials **337–339** (2005) 732.
[23]. Maddison, G. et al., Nuclear Fusion **51** (2011) 042001.
[24]. Giroud, C. et al., EX/P5-30, this conference .
[25]. Martin, Y.R. et al., Journal of Physics: Conference Series **123** (2008) 12033.
[26]. Maggi, C. et al., Nuclear Fusion **50** (2010) 025023 (20pp).
[27]. Lang, P. Fit. et al., Nuclear Fusion **45** (2005) 502.
[28]. Kallenbach, A. et al., Plasma Science, IEEE Transactions on **40** (2012) 605 .
[29]. Petrie, T. et al., Journal of Nuclear Materials **415** (2011) S906.

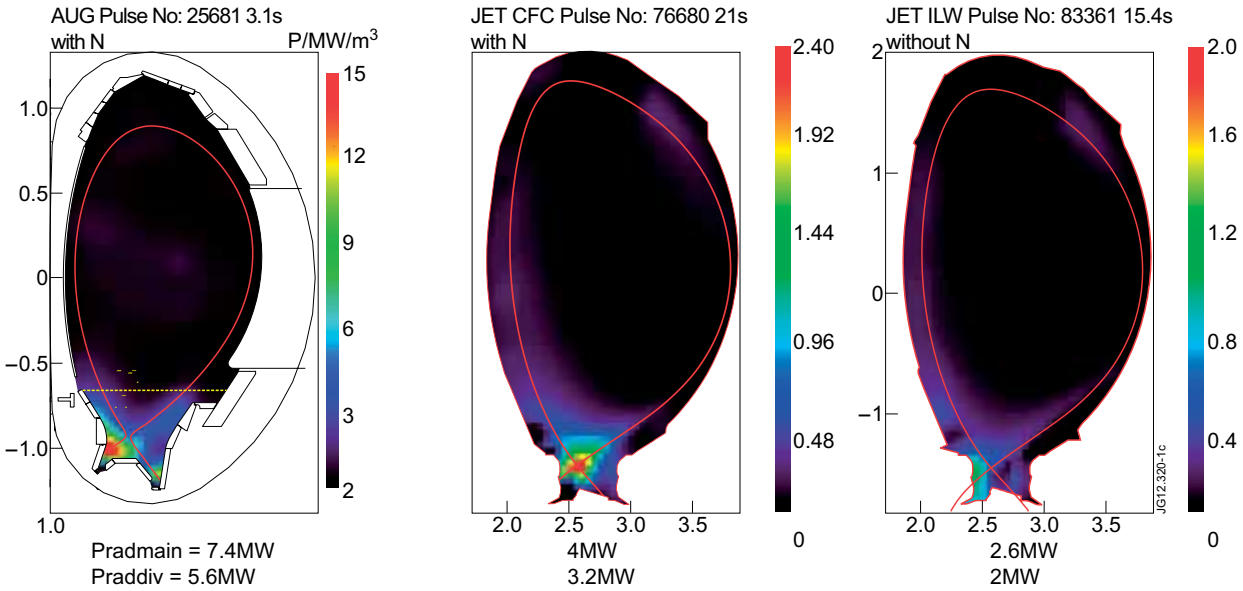

Figure 1: Tomographic reconstruction of the radiated power density in a N-seeded AUG discharge (ELM-averaged due to low time resolution of foil bolometers), and N-seeded JET-C discharges with carbon plasma facing components and an unseeded JET discharge with the ITER-like wall (both inter-ELM). The deconvolutions shown were done with an improved version of the 'Anisotropic Diffusion Model Tomography' algorithm [9]. Divertor radiation in AUG is dened as the radiation emitted below $z < -0.68$m, for JET $z < -1.2$m, accordingly. $P_{heat} \approx 14$MW.

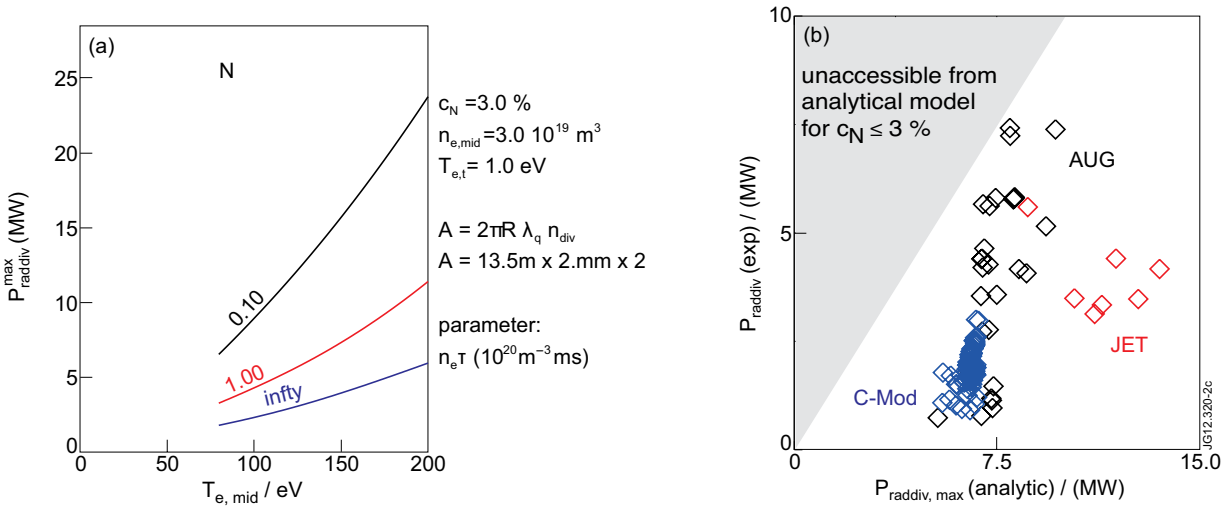

Figure 2: a) Maximum (i.e. for zero remaining heat ux to the target) divertor radiated power from the analytical 2-point divertor model, evaluated for typical AUG conditions and a nitrogen concentration of 3%. The parameter $n_e\tau$ is in the range 0.1–1 under the present conditions [7]. b) Measured divertor radiation in the database versus the maximum divertor radiated power for an edge nitrogen concentration of 3 % and $n_e\tau = 1$.

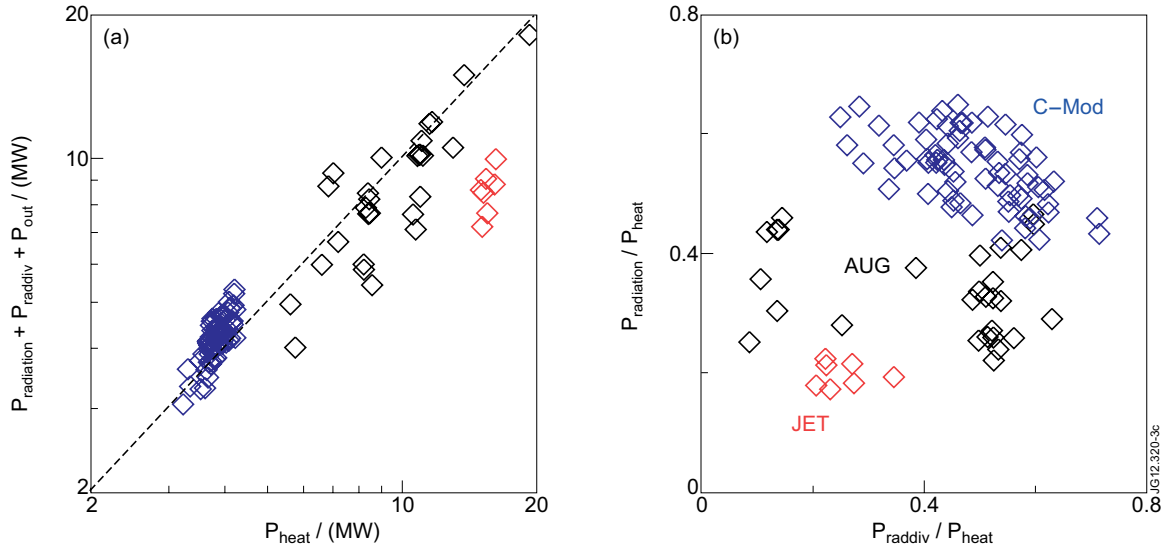

Figure 3: Characterisation of the present database. a) approximate power balance, omitting the inner target. b) main chamber versus divertor radiated power fraction.

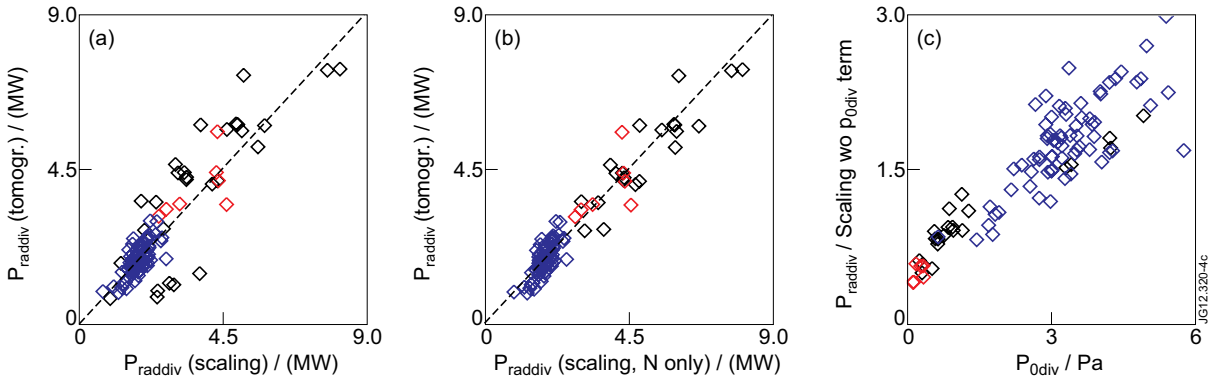

Figure 4: a) Measured divertor radiation versus the prediction of scaling Eq. 4. b) same versus scaling Eq. 5, only N seeded data. c) Divertor radiation, divided by scaling Eq.5 without the $p_{0,div}$ term, i.e. adjusted by the other dependencies, versus $p_{0,div}$, showing the pure neutral pressure dependence.

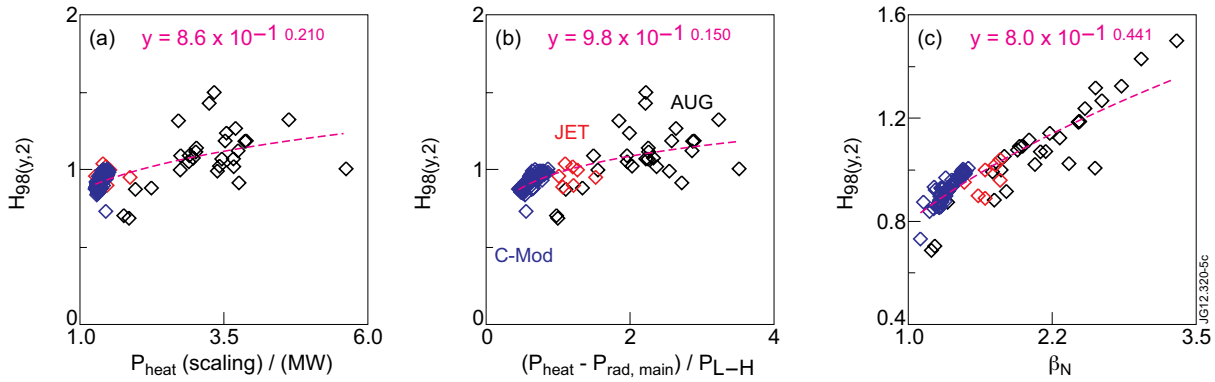

Figure 5: Normalised energy connement in terms of $H_{98(y,2)}$ versus a) the heating power normalized to the L-H power threshold [25], b) the power ux into the divertor normalized to the L-H power threshold, and c) versus β_N. The dotted lines show simple power law fits, with the coefcients plotted above.